Int. J. Heat Mass Transfer. Vol. 5, pp. 1149–1163. Pergamon Press 1962. Printed in Great Britain.

HEAT TRANSFER AND DIFFUSION IN WEDGE FLOWS WITH RAPID MASS TRANSFER

WARREN E. STEWART and RICHARD PROBER
Chemical Engineering Department, University of Wisconsin, Madison, Wisconsin

(*Received* 1 *August* 1961 *and in revised form* 4 *June* 1962)

Abstract—Boundary-layer solutions are given for the flow of binary constant-property mixtures over planes and wedges, with heat and mass transfer through the boundary surface. Exact numerical solutions are given for Prandtl and Schmidt numbers from 0·1 to 10. Asymptotic solutions are given for Prandtl and Schmidt numbers outside this range, and also for high rates of mass transfer toward the surface.

NOMENCLATURE

Symbols used more than once are listed below. Dimensions are given in terms of mass (M), length (L), time (t), and temperature (T). Any consistent units may be used.

$\hat{C}_p$,	Specific heat of the mixture; $(ML^2t^{-2})M^{-1}T^{-1}$;
$\mathscr{D}_{AB}$,	binary diffusivity, L^2t^{-1};
D^*	$= \delta^* \sqrt{\left(\frac{m+1}{2}\frac{U}{\nu x}\right)}$, boundary-layer displacement parameter, dimensionless;
D_0, D_1,	dimensionless coefficients in equation (39) and Table 2;
F, G, H,	dimensionless coefficients in equation (50) and Table 2;
G_3, G_4, G_5,	dimensionless quantities defined in equation (43);
I_0, I_3, etc.,	integrals in equations (44, 45) and Table 3;
$J^{\star}_{A0}$	$= N_{A0} - x_{A0}(N_{A0} + N_{B0})$, diffusion flux of species A into the boundary layer at $y = 0$ in a two-component system, moles $L^{-2}t^{-1}$;
K,	dimensionless mass-transfer rate defined in equation (11);
K_∞,	dimensionless mass-transfer rate defined in equation (43);
N_{A0},	total flux of species A into the boundary layer at $y = 0$, referred to stationary co-ordinates, moles $L^{-2}t^{-1}$;
Pr	$= \hat{C}_p\mu/k$, Prandtl number;
R_v, R_T, R_{AB},	dimensionless flux ratios. See equations (29, 30, 31);
Sc	$= \mu/\rho\mathscr{D}_{AB}$, Schmidt number for a binary mixture;
T,	temperature;
U	$= U(x)$, potential flow velocity at the edge of the boundary layer, Lt^{-1};
c,	molar density of the fluid, moles L^{-3};
f	$= \left(\frac{2}{m+1} U\nu x\right)^{-1/2} \int_{0,0}^{x,y} (u\mathrm{d}y - v\mathrm{d}x)$, dimensionless stream function;
$f''(0)$	$= f''(0, \beta, K)$, dimensionless velocity gradient at the wall;
$\mathrm{f}^{\bullet}$,	momentum-transfer coefficient, dimensionless. See equation (21);
$h^{\bullet}$,	heat-transfer coefficient, $(ML^2t^{-2})L^{-2}t^{-1}T^{-1}$ see equation (22);
$k^{\bullet}_x$,	diffusional transfer coefficient or "mass transfer coefficient," moles $L^{-2}t^{-1}$ (mole fraction)$^{-1}$. See equation (23);
k,	thermal conductivity of the fluid, $(ML^2t^{-2})L^{-1}t^{-1}T^{-1}$;

m, exponent in equation (1), dimensionless;
q_0, conductive heat flux into the boundary layer at $y = 0$, $(ML^2t^{-2})L^{-2}t^{-1}$;
u, v, velocity components in x and y directions in constant-property fluid, Lt^{-1};
u_1, value of U at $x = 1$;
w, dummy variable in equations (42) and (44);
x, distance downstream from the leading edge or stagnation point, L;
x_A, x_B, mole fractions in a binary mixture;
y, distance into the fluid, measured normal to the wall, L.

Greek symbols

Λ, Prandtl or Schmidt number, dimensionless.
$\Lambda_T = Pr$, $\Lambda_{AB} = Sc$;
Π, dimensionless temperature or composition:
$\Pi_T = (T - T_0)/(T_\infty - T_0)$,
$\Pi_{AB} = (x_A - x_{A0})/(x_{A\infty} - x_{A0})$;
$\Pi'(0)$ $= \Pi'(0, \beta, K, \Lambda)$, dimensionless gradient of temperature or composition at the wall;
α $= k/\rho\hat{C}_p$, thermal diffusivity, L^2t^{-1};
β $= 2m/(m + 1)$, angle parameter illustrated in Fig. 1;
δ^* $= \int_0^\infty \left(1 - \frac{u}{U}\right) \mathrm{d}y$, boundary-layer displacement thickness, L;
δ_p, total displacement distance for streamlines in the adjacent potential flow, L, see equation (40);
η, dimensionless position coordinate, see equation (12);
μ, viscosity of the fluid, $ML^{-1}t^{-1}$;
ν $= \mu/\rho$, kinematic viscosity of the fluid, L^2t^{-1};
π, 3·14159 . . .;
ρ, density of the fluid, ML^{-3};
τ_0, wall shear stress, $(MLt^{-2})L^{-2}$.

Superscripts

$'$ $= \mathrm{d}/\mathrm{d}\eta$;
$\star$, denotes a flux relative to the molar average velocity of the mixture;
$*$, denotes a conventional displacement thickness;
$\bullet$, denotes a transfer coefficient evaluated at the prevailing mass transfer conditions.

Subscripts

0, evaluated at $\eta = 0$;
∞, evaluated at $\eta = \infty$ (except for K_∞, which appears in an asymptotic solution for $\Lambda \to \infty$);
A or B, evaluated for species A or B in a binary mixture.

Functions

$$\mathrm{erf}\,(a) = \frac{2}{\sqrt{\pi}} \int_0^a \mathrm{e}^{-x^2}\,\mathrm{d}x = -\,\mathrm{erf}\,(-a).$$

1. INTRODUCTION

When rapid mass transfer occurs through an interface or porous surface, the usual condition of zero velocity at the surface does not apply. Instead, one or more chemical species flow through the surface, and these flows lead to a variety of effects. In particular, the transfer coefficients, the stability of laminar flow, and the possibility of separation in decelerated flows, all depend on the mass transfer rate. These effects are exploited in boundary layer control and transpiration cooling; they also occur in heterogeneous catalysis, combustion and other diffusional operations.

Mass transfer is defined here as the transfer of one or more chemical species through an interface or porous wall. Diffusion is defined as the motion of two or more chemical species in a mixture relative to one another. It should be noted that mass transfer is usually accompanied by diffusion, but there are important exceptions; for example, the condensation of pure steam involves mass transfer but no diffusion.

The groundwork for an accurate fluid-mechanical description of forced-convection mass transfer was provided by the work of Schlichting and Bussmann [1] and Schaefer [2] on velocity profiles around porous-walled wedges. More recently, there have been many theoretical investigations of mass transfer effects in wedge flows; space permits mentioning only a few here.

The first exact boundary-layer calculations for heat transfer in the presence of mass transfer were made by Eckert [3]; the corresponding diffusional problem was first treated by Schuh [4]. Transpiration-cooling calculations for air with temperature-dependent properties were made by Brown and Donoughe [5]. Methods for adapting wedge flow mass transfer solutions to other geometries were given by Eckert and Livingood [6], Spalding [7], and Spalding and Evans [8, 9]. The theory of injection cooling of porous wedges in high-speed flow, with liquid or gaseous coolant, was treated by Hartnett and Eckert [10]. These and other exact solutions for wedge flow with mass transfer are published in [1–16].

The influence of the Prandtl and Schmidt numbers (Λ_T and Λ_{AB} in the present notation) in wedge flows with rapid mass transfer has not been adequately studied. Exact solutions are known only for Λ near unity. Asymptotic solutions are available for large values of Λ [17, 12, 15, 14, 9] but their accuracy for finite Λ has not been adequately tested. The need for additional exact solutions has been emphasized recently by Spalding and Evans [7, 8, 9, 18], who have also discussed possible applications in some detail.

The purpose of the present work is to provide accurate solutions for heat transfer and diffusion over the whole range of Λ (zero to infinity), and for various wedge geometries and mass transfer rates. With these solutions, practical calculations can be made not only for gaseous systems, ($\Lambda \simeq 1$) but also for molten metals ($\Lambda \ll 1$) and other Newtonian liquids ($\Lambda \gg 1$).

2. FORMULATION OF THE PROBLEM

Consider the steady two-dimensional flow of a pure or binary fluid as shown in Fig. 1(a) or 1(b). Viscous dissipation and chemical reactions in the fluid are neglected. The fluxes of momentum, heat, and matter at the wall are to be found from the constant-property boundary-layer equations,

$$\frac{\partial u}{\partial x} + \frac{\partial v}{\partial y} = 0 \tag{1}$$

$$u\frac{\partial u}{\partial x} + v\frac{\partial u}{\partial y} = U\frac{\mathrm{d}U}{\mathrm{d}x} + \nu\frac{\partial^2 u}{\partial y^2} \tag{2}$$

$$u\frac{\partial T}{\partial x} + v\frac{\partial T}{\partial y} = \alpha\frac{\partial^2 T}{\partial y^2} \tag{3}$$

$$u\frac{\partial x_A}{\partial x} + v\frac{\partial x_A}{\partial y} = \mathscr{D}_{AB}\frac{\partial^2 x_A}{\partial y^2} \tag{4}$$

under the boundary conditions,

as $y \to \infty$:

$$u \to U(x) = u_1 x^m \tag{5}$$

$$T \to T_\infty \tag{6}$$

$$x_A \to x_{A\infty}. \tag{7}$$

At $y = 0$:

$$u = 0 \tag{8}$$

$$T = T_0 \tag{9}$$

$$x_A = x_{A0} \tag{10}$$

$$v = v_0(x) = K\sqrt{\left(\frac{m+1}{2}\,\nu\, u_1 x^{m-1}\right)} \tag{11}$$

in which u_1, T_∞, $x_{A\infty}$, T_0, x_{A0} and K are independent of x. The mass transfer distribution in equation (11) was selected to simplify the subsequent analysis; it also corresponds to the important practical cases of constant N_{A0}/q_0 and N_{A0}/N_{B0} along the wall (see Section 3).

It is well known [9, 10, 16] that the above two-dimensional problem can be made one-dimensional by introducing the position coordinate

$$\eta = y\sqrt{\left(\frac{m+1}{2}\,\frac{U}{\nu x}\right)} \tag{12}$$

and that the velocity field in the boundary layer is then determined by the differential equation

$$f''' + f'' + \beta(1 - f'^2) = 0 \tag{13}$$

with the boundary conditions

$$\text{as} \quad \eta \to \infty \quad f' \to 1 \tag{14}$$

$$\text{at} \quad \eta = 0 \quad f' = 0 \tag{15}$$

$$\text{at} \quad \eta = 0 \quad f = -K. \tag{16}$$

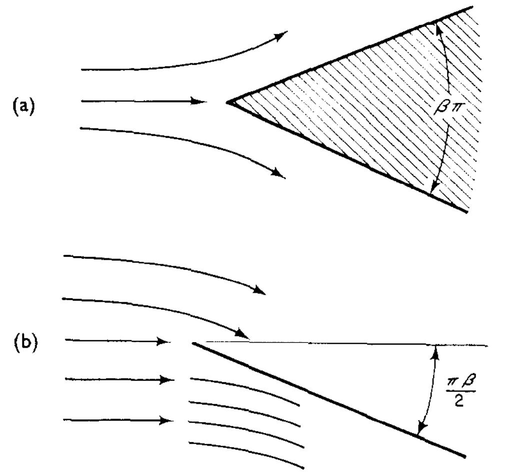

FIG. 1. Flow geometries
(a) Two-dimensional wedge (positive β)
(b) Obliquely mounted plate (negative β) with flow control on the bottom side. The region of interest is above the plate.

Correspondingly, the temperature and composition fields are each determined by a differential equation of the form

$$\Pi'' + \Lambda f \Pi' = 0 \tag{17}$$

with the boundary conditions

$$\text{as} \quad \eta \to \infty \quad \Pi \to 1 \tag{18}$$

$$\text{at} \quad \eta = 0 \quad \Pi = 0. \tag{19}$$

Here Π is a dimensionless temperature or composition, and Λ is the Prandtl or Schmidt number. The analogy between the thermal and diffusional problems is evident.

3. NUMERICAL SOLUTIONS OF THE DIFFERENTIAL EQUATIONS

Solutions of equations (13–19) were computed at mass transfer rates from $K = -5$ to $K = +3$ and for angles, $\pi\beta$, from $-\pi$ to π. Separation conditions were explored in detail, and are shown in Fig. 2. The separation boundary joins the line $\beta = 0$ smoothly at the "blow-off" condition $K = 1{\cdot}23849/\sqrt{2}$, given by Emmons and Leigh [11]; for K above this value at $\beta = 0$ no steady flow solution exists.

At each combination of β and K, the f-profile was first computed; this involved a series of trial integrations to determine the dimensionless velocity gradient at the wall, $f''(0)$. The computed f-profile was then inserted in equation (17) and Π-profiles were computed for various values of Λ.

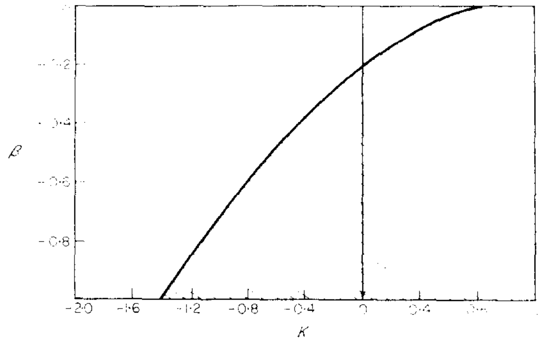

FIG. 2. Separation conditions in decelerated flow. The shaded region includes separated and unsteady flows.

The numerical results for the transfer coefficients and wall fluxes are given in Table 1. These results include the dimensionless velocity gradient at the wall, $f''(0)$; the dimensionless temperature or concentration gradient at the wall, $\Pi'(0)$; and a set of auxiliary quantities R_v, R_T and R_{AB} which will be discussed presently. The values of $\Pi'(0)$ were computed from

$$\frac{1}{\Pi'(0)} = \int_0^\infty \exp\left\{-\Lambda \int_0^\eta f\, d\eta\right\} dn. \tag{20}$$

The results are believed correct within 0·5 in the last digit, except for $f''(0)$ and β which are given unrounded and may be uncertain by several units in the last digit. Asymptotic solutions for conditions outside the range of this table are given in the next section.

In compiling Table 1 a number of values obtainable from [1–14] have been recalculated. In such cases the tabulated values of $f''(0)$ and $\Pi'(0)$ have generally shown at least 3-figure agreement with earlier work.

The local transfer coefficients or fluxes at any point on the wall can be computed from Table 1 and the relations

β	K	$f''(0)$	R_v	$\Lambda = 0{\cdot}1$ $\Pi'(0)$	R	$\Lambda = 0{\cdot}2$ $\Pi'(0)$	R	Λ $\Pi'(0)$
1·0	−5·0	5·3595395	−0·93291597	0·6213	−0·8048	1·1291	−0·8857	2·6195
	−3·0	3·5266402	−0·85066801	0·4510	−0·6652	0·7716	−0·7776	1·6753
	−1·0	1·8891	−0·5293	0·2926	−0·3418	0·4423	−0·4522	0·8017
	−0·5	1·5417	−0·3243	0·2554	−0·1957	0·3672	−0·2723	0·6084
	−0·2	1·3511	−0·1480	0·2337	$-8{\cdot}557\times10^{-2}$	0·3241	−0·1234	0·5008
	−0·1	1·2910	−0·07746	0·2266	$-4{\cdot}413\times10^{-2}$	0·3101	$6{\cdot}449\times10^{-2}$	0·4666
	0	1·2326	0·0	0·2195	0·0	0·2963	0·0	0·4333
	0·1	1·1760	0·08503	0·2125	$4{\cdot}706\times10^{-2}$	0·2828	$7{\cdot}073\times10^{-2}$	0·4011
	0·2	1·1214	0·1784	0·2055	$9{\cdot}732\times10^{-2}$	0·2694	0·1485	0·3698
	0·5	0·9692	0·5159	0·1850	0·2702	0·2307	0·4334	0·2828
	1·0	0·7566	1·3218	0·1525	0·6559	0·1718	1·1641	0·1639
	2·0	0·47581055	4·2033536	$9{\cdot}5358\times10^{-2}$	2·0974	$8{\cdot}0111\times10^{-2}$	4·9931	$3{\cdot}3053\times10^{-[illegible]}$
	3·0	0·32945314	9·1059991	$5{\cdot}25\times10^{-2}$	5·71	$2{\cdot}79\times10^{-2}$	$2{\cdot}15\times10^{1}$	$2{\cdot}74\times10^{-3}$
0·5	−5·0	5·2304013	−0·95594959	0·6211	−0·8051	1·1285	−0·8861	2·6185
	−3·0	3·3458260	−0·89663957	0·4501	−0·6665	0·7700	−0·7792	1·6725
	−1·0	1·6241995	−0·61568791	0·2895	−0·3454	0·4369	−0·4578	0·7912
	−0·5	1·2540	−0·3987	0·2510	−0·1992	0·3595	−0·2781	0·5935
	−0·2	1·0521	−0·1901	0·2282	$-8{\cdot}763\times10^{-2}$	0·3147	−0·1271	0·4827
	−0·1	0·9888	−0·1011	0·2207	$-4{\cdot}531\times10^{-2}$	0·3000	$6{\cdot}666\times10^{-2}$	0·4473
	0	0·9277	0·0	0·2132	0·0	0·2856	0·0	0·4129
	0·1	0·8689	0·1151	0·2057	$4{\cdot}862\times10^{-2}$	0·2712	$7{\cdot}373\times10^{-2}$	0·3794
	0·2	0·8126	0·2461	0·1982	0·1009	0·2571	0·1556	0·3470
	0·5	0·6594	0·7583	0·1761	0·2839	0·2160	0·4629	0·2568
	1·0	0·4604	2·1719	0·1404	0·7121	0·1531	1·3062	0·1353
	2·0	0·24978729	8·0068125	$7{\cdot}879\times10^{-2}$	2·538	$5{\cdot}937\times10^{-2}$	6·737	$1{\cdot}772\times10^{-2}$
	3·0	0·16666654	$1{\cdot}8000014\times10^{1}$	$3{\cdot}70\times10^{-2}$	8·11	$1{\cdot}51\times10^{-2}$	$3{\cdot}96\times10^{2}$	$6{\cdot}53\times10^{-4}$
0	−5·0	5·0942987	−0·98148937	0·6206	−0·8057	1·1279	−0·8866	2·6174
	−3·0	3·145101	−0·95386444	0·4491	−0·6680	0·7681	−0·7811	1·6691
	−1·0	1·283634	−0·7790383	0·2846	−0·3514	0·4282	−0·4671	0·7746
	−0·5	0·8579	−0·5828	0·2427	−0·2060	0·3452	−0·2896	0·5664
	−0·2	0·6190	−0·3231	0·2165	$-9{\cdot}239\times10^{-2}$	0·2948	−0·1357	0·4456
	−0·1	0·5432	−0·1841	0·2074	$-4{\cdot}822\times10^{-2}$	0·2777	$-7{\cdot}202\times10^{-2}$	0·4060
	0	0·46960002	0·0	0·1980	0·0	0·2604	0·0	0·3667
	0·1	0·39859059	0·25088400	0·1884	$5{\cdot}308\times10^{-2}$	0·2427	$8{\cdot}241\times10^{-2}$	0·3277
	0·2	0·3305	0·6051	0·1783	0·1121	0·2246	0·1781	0·2890
	0·5	0·1485	3·3672	0·1441	0·3470	0·1658	0·6033	0·1736
	0·75	$3{\cdot}401\times10^{-2}$	$2{\cdot}205\times10^{1}$	0·1032	0·7270	0·1023	1·4662	$7{\cdot}347\times10^{-2}$
	0·825	$1{\cdot}0428078\times10^{-2}$	$7{\cdot}9113332\times10^{1}$	$8{\cdot}1705\times10^{-2}$	1·0097	$7{\cdot}2758\times10^{-2}$	2·2678	$3{\cdot}8540\times10^{-[illegible]}$
	0·85	$4{\cdot}4310057\times10^{-3}$	$1{\cdot}9183004\times10^{2}$	$6{\cdot}991\times10^{-2}$	1·216	$5{\cdot}779\times10^{-2}$	2·942	$2{\cdot}451\times10^{-2}$
	0·875	$6{\cdot}793121\times10^{-5}$	$1{\cdot}2880677\times10^{4}$	$3{\cdot}630\times10^{-2}$	2·410	$2{\cdot}120\times10^{-2}$	8·254	$2{\cdot}906\times10^{-3}$
−0·009115	0·75	0·0	∞	$8{\cdot}134\times10^{-2}$	0·9220	$7{\cdot}316\times10^{-2}$	2·0504	$4{\cdot}016\times10^{-2}$
−0·050178	0·5	0·0	∞	0·1155	0·4331	0·1232	0·8114	0·1094
−0·100000	0	0·31926989	0·0	0·1904	0·0	0·2480	0·0	0·3445
	0·299685	0·0	∞	0·1361	0·2203	0·1570	0·3819	0·1698
−0·162793	−1·0	1·1424	−0·8754	0·2821	−0·3545	0·4238	−0·4719	0·7665
	−0·5	0·6734	−0·7425	0·2375	−0·2105	0·3365	−0·2972	0·5503
	−0·2	0·3898	−0·5131	0·2072	$-9{\cdot}654\times10^{-2}$	0·2794	−0·1432	0·4176
	−0·1	0·2908	−0·3438	0·1954	$-5{\cdot}118\times10^{-2}$	0·2580	$-7{\cdot}751\times10^{-2}$	0·3706
	0	0·1832	0·0	0·1815	0·0	0·2335	0·0	0·3190
	0·1	0·0	∞	0·1546	$6{\cdot}470\times10^{-2}$	0·1890	0·1058	0·2348
−0·198838	0	0·0	∞	0·1634	0·0	0·2048	0·0	0·2690
−0·200000	−3·0	3·0576278	−0·98115277	0·4486	−0·6688	0·7673	−0·7820	1·6675
	−1·0	1·1066908	−0·90359475	0·2814	−0·3554	0·4227	−0·4732	0·7643
	−0·5	0·62291361	−0·80267952	0·2360	−0·2119	0·3338	−0·2995	0·5453
	−0·2	0·31759557	−0·62973171	0·2036	$-9{\cdot}824\times10^{-2}$	0·2735	−0·1463	0·4069
	−0·1	0·20066407	−0·49834532	0·1897	$-5{\cdot}270\times10^{-2}$	0·2489	$-8{\cdot}037\times10^{-2}$	0·3542
	−0·00309208	0·0	−∞	0·1637	$-1{\cdot}889\times10^{-3}$	0·2053	$-3{\cdot}013\times10^{-3}$	0·2701
−0·237842	−0·1	0·0	−∞	0·1720	$-5{\cdot}813\times10^{-2}$	0·2205	$-9{\cdot}070\times10^{-2}$	0·3043
−0·422021	−0·5	0·0	−∞	0·2055	−0·2433	0·2835	−0·3527	0·4546
−0·500000	−0·64596487	0·0	−∞	0·2175	−0·2970	0·3068	−0·4211	0·5126
−0·712061	−1·0	0·0	−∞	0·2464	−0·4059	0·3638	−0·5497	0·6589
−1·000000	−1·4142136	0·0	−∞	0·2802	−0·5048	0·4321	−0·6546	0·8383

n for the transfer coefficients and wall fluxes.

0·5 R	$\Lambda = 0{\cdot}7$ $\Pi'(0)$	R	$\Lambda = 1{\cdot}0$ $\Pi'(0)$	R	Λ $\Pi'(0)$
−0·95438	3·6098	−0·96958	5·0968	−0·98101	$1{\cdot}00679 \times 10^{1}$
−0·8953	2·2672	−0·92623	3·1531	−0·95143	6·1145
−0·6237	1·0160	−0·6889	1·3234	−0·7556	2·3073
−0·4109	0·7409	−0·4724	0·9216	−0·5425	1·4595
−0·1997	0·5895	−0·2375	0·7033	−0·2844	1·0081
−0·1072	0·5418	−0·1292	0·6354	−0·1574	0·8716
0·0	0·4958	0·0	0·5704	0·0	0·7435
0·1247	0·4515	0·1550	0·5085	0·1967	0·6249
0·2704	0·4090	0·3423	0·4497	0·4447	0·5163
0·8839	0·2933	1·1932	0·2950	1·6951	0·2580
3·0512	0·1456	4·8063	0·1168	8·5649	$4{\cdot}780 \times 10^{-2}$
$3{\cdot}0254 \times 10^{1}$	$1{\cdot}6658 \times 10^{-2}$	$8{\cdot}4045 \times 10^{1}$	$5{\cdot}5959 \times 10^{-3}$	$3{\cdot}5741 \times 10^{2}$	$1{\cdot}1586 \times 10^{-4}$
$5{\cdot}47 \times 10^{2}$	$5{\cdot}15 \times 10^{-4}$	$4{\cdot}08 \times 10^{3}$	$3{\cdot}88 \times 10^{-5}$	$7{\cdot}73 \times 10^{4}$	$5{\cdot}46 \times 10^{-9}$
−0·95475	3·6087	−0·96988	5·0956	−0·98124	$1{\cdot}00668 \times 10^{1}$
−0·8969	2·2639	−0·92759	3·1494	−0·95255	6·1108
−0·6320	1·0031	−0·6978	1·3078	−0·7646	2·2874
−0·4212	0·7223	−0·4846	0·8986	−0·5564	1·4269
−0·2072	0·5669	−0·2470	0·6752	−0·2962	0·9668
−0·1118	0·5179	−0·1352	0·6056	−0·1651	0·8276
0·0	0·4705	0·0	0·5389	0·0	0·6972
0·1318	0·4248	0·1648	0·4754	0·2103	0·5768
0·2882	0·3810	0·3675	0·4153	0·4816	0·4672
0·9735	0·2622	1·3347	0·2583	1·9357	0·2125
3·6947	0·1148	6·0959	$8{\cdot}595 \times 10^{-2}$	$1{\cdot}163 \times 10^{1}$	$2{\cdot}784 \times 10^{-2}$
$5{\cdot}643 \times 10^{1}$	$7{\cdot}140 \times 10^{-3}$	$1{\cdot}961 \times 10^{2}$	$1{\cdot}703 \times 10^{-3}$	$1{\cdot}174 \times 10^{3}$	$1{\cdot}112 \times 10^{-5}$
$2{\cdot}30 \times 10^{3}$	$7{\cdot}00 \times 10^{-5}$	$3{\cdot}00 \times 10^{4}$	$2{\cdot}28 \times 10^{-6}$	$1{\cdot}32 \times 10^{6}$	$1{\cdot}93 \times 10^{-11}$
−0·95514	3·6075	−0·97021	5·0943	−0·98149	$1{\cdot}00656 \times 10^{1}$
−0·89871	2·2600	−0·92921	3·1451	−0·95386	6·1064
−0·6455	0·9829	−0·7122	1·2836	−0·7790	2·2568
−0·4414	0·6890	−0·5080	0·8579	−0·5829	1·3705
−0·2244	0·5213	−0·2686	0·6190	−0·3231	0·8860
−0·1232	0·4671	−0·1499	0·5432	−0·1841	0·7373
0·0	0·4139	0·0	0·4696	0·0	0·5972
0·1526	0·3618	0·1935	0·3986	0·2509	0·4674
0·3460	0·3108	0·4505	0·3305	0·0651	0·3497
1·4403	0·1656	2·1137	0·1485	3·3672	$9{\cdot}097 \times 10^{-2}$
5·1040	$5{\cdot}493 \times 10^{-2}$	9·5575	$3{\cdot}401 \times 10^{-2}$	$2{\cdot}205 \times 10^{1}$	$5{\cdot}708 \times 10^{-3}$
$1{\cdot}0703 \times 10^{1}$	$2{\cdot}3364 \times 10^{-2}$	$2{\cdot}4718 \times 10^{1}$	$1{\cdot}0428 \times 10^{-2}$	$7{\cdot}911 \times 10^{1}$	$5{\cdot}571 \times 10^{-4}$
$1{\cdot}734 \times 10^{1}$	$1{\cdot}269 \times 10^{-2}$	$4{\cdot}687 \times 10^{1}$	$4{\cdot}431 \times 10^{-3}$	$1{\cdot}918 \times 10^{2}$	$1{\cdot}015 \times 10^{-4}$
$1{\cdot}505 \times 10^{2}$	$6{\cdot}716 \times 10^{-4}$	$9{\cdot}119 \times 10^{2}$	$6{\cdot}793 \times 10^{-5}$	$1{\cdot}288 \times 10^{4}$	$2{\cdot}402 \times 10^{-8}$
9·3380	$2{\cdot}498 \times 10^{-2}$	$2{\cdot}102 \times 10^{1}$	$1{\cdot}160 \times 10^{-2}$	$6{\cdot}464 \times 10^{1}$	$7{\cdot}090 \times 10^{-4}$
2·2851	$9{\cdot}459 \times 10^{-2}$	3·7001	$7{\cdot}340 \times 10^{-2}$	6·8118	$2{\cdot}742 \times 10^{-2}$
0·0	0·3870	0·0	0·4368	0·0	0·5504
0·8825	0·1665	1·2600	0·1561	1·9194	0·1127
−0·6523	0·9731	−0·7193	1·2720	−0·7861	2·2425
−0·4543	0·6693	−0·5230	0·8339	−0·5996	1·3382
−0·2395	0·4870	−0·2874	0·5772	−0·3465	0·8267
−0·1349	0·4239	−0·1651	0·4905	−0·2039	0·6620
0·0	0·3561	0·0	0·3993	0·0	0·4968
0·2130	0·2500	0·2800	0·2638	0·3790	0·2788
0·0	0·2956	0·0	0·3258	0·0	0·3915
−0·8996	2·2582	−0·92995	3·1431	−0·95446	6·1045
−0·6542	0·9705	−0·7213	1·2690	−0·7880	2·2387
−0·4584	0·6633	−0·5277	0·8267	−0·6048	1·3284
−0·2458	0·4740	−0·2953	0·5614	−0·3563	0·8042
−0·1412	0·4041	−0·1732	0·4663	−0·2145	0·6273
$-5{\cdot}725 \times 10^{-3}$	0·2970	$-7{\cdot}287 \times 10^{-3}$	0·3278	$-9{\cdot}433 \times 10^{-3}$	0·3952
−0·1643	0·3434	−0·2038	0·3924	−0·2549	0·5207
−0·5500	0·5533	−0·6326	0·6945	−0·7199	1·1536
−0·6301	0·6358	−0·7112	0·8155	−0·7921	1·4131
−0·7588	0·8456	−0·8279	1·1246	−0·8892	2·0733
−0·8435	1·1037	−0·8970	1·5050	−0·93968	2·8740

= 2·0	$\Lambda = 5{\cdot}0$		$\Lambda = 10{\cdot}0$	
R	$\Pi'(0)$	R	$\Pi'(0)$	R
−0·99325	$2{\cdot}5035\times10^{1}$	−0·99860	$5{\cdot}0019\times10^{1}$	−0·999613
−0·98127	$1{\cdot}5062\times10^{1}$	−0·99586	$3{\cdot}00350\times10^{1}$	−0·998835
−0·8668	5·2236	−0·95720	$1{\cdot}0138\times10^{1}$	−0·98630
−0·6852	2·9331	−0·8523	5·3446	−0·93553
−0·3968	1·7171	−0·5824	2·7370	−0·7307
−0·2295	1·3623	−0·3670	1·9869	−0·5033
0·0	1·0428	0·0	1·3373	0·0
0·3200	0·7652	0·6534	0·8173	1·2236
0·7747	0·5334	1·8749	0·4412	4·5334
3·8763	0·1228	$2{\cdot}035\times10^{1}$	$2{\cdot}704\times10^{-2}$	$1{\cdot}849\times10^{2}$
$4{\cdot}184\times10^{1}$	$2{\cdot}08\times10^{-3}$	$2{\cdot}41\times10^{3}$	$7{\cdot}42\times10^{-6}$	$1{\cdot}35\times10^{6}$
$3{\cdot}4525\times10^{4}$	$5{\cdot}671\times10^{-10}$	$1{\cdot}763\times10^{10}$	$5{\cdot}24\times10^{-19}$	$3{\cdot}82\times10^{19}$
$1{\cdot}10\times10^{9}$	$8{\cdot}43\times10^{-21}$	$1{\cdot}78\times10^{21}$	$1{\cdot}14\times10^{-40}$	$2{\cdot}62\times10^{41}$
−0·93337	$2{\cdot}5034\times10^{1}$	−0·99863	$5{\cdot}00189\times10^{1}$	−0·999622
−0·98187	$1{\cdot}5060\times10^{1}$	−0·99603	$3{\cdot}00334\times10^{1}$	−0·998890
−0·8744	5·2052	−0·96058	$1{\cdot}0131\times10^{1}$	−0·98706
−0·7008	2·8900	−0·8651	5·3013	−0·94316
−0·4137	1·6542	−0·6045	2·6578	−0·7525
−0·2417	1·2935	−0·3865	1·8951	−0·5277
0·0	0·9699	0·0	1·2380	0·0
0·3467	0·6911	0·7235	0·7201	1·3887
0·8561	0·4625	2·1623	0·3600	5·5554
4·7049	$8{\cdot}489\times10^{-2}$	$2{\cdot}945\times10^{1}$	$1{\cdot}376\times10^{-2}$	$3{\cdot}634\times10^{2}$
$7{\cdot}184\times10^{1}$	$5{\cdot}805\times10^{-4}$	$8{\cdot}613\times10^{3}$	$6{\cdot}02\times10^{-7}$	$1{\cdot}663\times10^{7}$
$3{\cdot}597\times10^{6}$	$1{\cdot}70\times10^{-12}$	$5{\cdot}90\times10^{12}$	$4{\cdot}8\times10^{-24}$	$4{\cdot}2\times10^{24}$
$3{\cdot}11\times10^{11}$	$6{\cdot}5\times10^{-27}$	$2{\cdot}31\times10^{21}$	$6{\cdot}9\times10^{-53}$	$4{\cdot}3\times10^{53}$
−0·99348	$2{\cdot}5034\times10^{1}$	−0·99866	$5{\cdot}00185\times10^{1}$	−0·999631
−0·98257	$1{\cdot}5057\times10^{1}$	−0·99623	$3{\cdot}00315\times10^{1}$	−0·998951
−0·8862	5·1747	−0·96624	$1{\cdot}01080\times10^{1}$	−0·98931
−0·7296	2·8186	−0·8870	5·2329	−0·95549
−0·4515	1·5344	−0·6517	2·5108	−0·7965
−0·2713	1·1552	−0·4328	1·7134	−0·5836
0·0	0·8156	0·0	1·0297	0·0
0·4279	0·5271	0·9486	0·5105	1·9588
1·1440	0·3015	3·3168	0·1905	$1{\cdot}050\times10^{1}$
$1{\cdot}099\times10^{1}$	$1{\cdot}467\times10^{-2}$	$1{\cdot}704\times10^{2}$	$4{\cdot}88\times10^{-4}$	$1{\cdot}025\times10^{4}$
$2{\cdot}628\times10^{2}$	$1{\cdot}52\times10^{-5}$	$2{\cdot}47\times10^{5}$	$4{\cdot}9\times10^{-10}$	$1{\cdot}5\times10^{10}$
$2{\cdot}962\times10^{3}$	$4{\cdot}46\times10^{-8}$	$9{\cdot}24\times10^{7}$	$4{\cdot}2\times10^{-15}$	$1{\cdot}9\times10^{15}$
$1{\cdot}675\times10^{4}$	$6{\cdot}31\times10^{-10}$	$6{\cdot}74\times10^{9}$	$8{\cdot}4\times10^{-19}$	$1{\cdot}01\times10^{19}$
$7{\cdot}287\times10^{7}$	$5{\cdot}41\times10^{-19}$	$8{\cdot}08\times10^{18}$	$6{\cdot}2\times10^{-37}$	$1{\cdot}4\times10^{37}$
$2{\cdot}116\times10^{3}$	$8{\cdot}445\times10^{-8}$	$4{\cdot}441\times10^{7}$	$1{\cdot}546\times10^{-14}$	$4{\cdot}852\times10^{14}$
$3{\cdot}647\times10^{1}$	$8{\cdot}930\times10^{-4}$	$2{\cdot}799\times10^{3}$	$1{\cdot}906\times10^{-6}$	$2{\cdot}623\times10^{6}$
0·0	0·7436	0·0	0·9327	0·0
5·3176	$3{\cdot}150\times10^{-2}$	$4{\cdot}756\times10^{1}$	$2{\cdot}734\times10^{-3}$	$1{\cdot}096\times10^{3}$
−0·8919	5·1609	−0·96882	$1{\cdot}0098\times10^{1}$	−0·99026
−0·7473	2·7795	−0·8994	5·1986	−0·96179
−0·4839	1·4482	−0·6905	2·4082	−0·8305
−0·3021	1·0410	−0·4803	1·5649	−0·6390
0·0	0·6611	0·0	0·8206	0·0
0·7172	0·2525	1·9799	0·1795	5·5718
0·0	0·4955	0·0	0·5905	0·0
−0·98289	$1{\cdot}50554\times10^{1}$	−0·996321	$3{\cdot}00294\times10^{1}$	−0·999022
−0·8934	5·1575	−0·96946	$1{\cdot}00954\times10^{1}$	−0·990547
−0·7528	2·7678	−0·90323	5·1880	−0·96376
−0·4974	1·4157	−0·7064	2·3699	−0·8439
−0·3188	0·9882	−0·5060	1·4961	−0·6684
$-1{\cdot}565\times10^{-2}$	0·5044	$-3{\cdot}065\times10^{-2}$	0·6081	$-5{\cdot}085\times10^{-2}$
−0·3841	0·8226	−0·6078	1·2781	−0·7824
−0·8669	2·5719	−0·97206	5·0236	−0·99530
−0·91426	3·2772	−0·98556	6·4755	−0·99756
−0·96466	5·0215	−0·99571	$1{\cdot}0006\times10^{1}$	−0·99936
−0·98416	7·0824	−0·99840	$1{\cdot}4145\times10^{1}$	−0·99977

$$\frac{f^{\bullet}}{2} = \frac{\tau_0}{\frac{1}{2}\rho U^2} = f''(0) \sqrt{\left(\frac{m+1}{2} \frac{\nu}{Ux}\right)} \quad (21)$$

$$\frac{h^{\bullet}}{\rho U \hat{C}_p} = \frac{q_0}{\rho U \hat{C}_p(T_0 - T_\infty)}$$

$$= \frac{\Pi'_T(0)}{Pr} \sqrt{\left(\frac{m+1}{2} \frac{\nu}{Ux}\right)} \quad (22)$$

$$\frac{k_x^{\bullet}}{cU} = \frac{N_{A0} - x_{A0}(N_{A0} + N_{B0})}{cU(x_{A0} - x_{A\infty})}$$

$$= \frac{\Pi'_{AB}(0)}{Sc} \sqrt{\left(\frac{m+1}{2} \frac{\nu}{Ux}\right)} \quad (23)$$

in which the black dots (•) signify that these transfer coefficients are evaluated at the prevailing mass transfer rate. The table is set up to handle known or unknown mass transfer rates; thus if K is known one interpolates as follows:

$$f''(0) = f''(0, \beta, K) \quad (24)$$

$$\Pi'(0) = \Pi'(0, \beta, K, \Lambda). \quad (25)$$

On the other hand, if K is unknown, one first finds K from Table 1 by means of *one* of the following tabulated functions:

$$K = K(\beta, R_v) \quad (26)$$

or

$$K = K(\beta, R_T, \Lambda_T) \quad (27)$$

or

$$K = K(\beta, R_{AB}, \Lambda_{AB}), \quad (28)$$

and then follows the procedure for known K. The quantities R_v, R_T, R_{AB} are defined as follows (for a binary constant-property system with no dissipation or chemical reaction):

$$R_v = \frac{v_0 \rho U}{\tau_0} \quad (29)$$

$$R_T = \frac{v_0 \rho \hat{C}_p (T_0 - T_\infty)}{q_0} \quad (30)$$

$$R_{AB} = \frac{v_0 c(x_{A0} - x_{A\infty})}{J^{\star}_{A0}}$$

$$= \frac{(x_{A0} - x_{A\infty})}{\dfrac{N_{A0} + N_{B0}}{N_{A0}} - x_{A0}}. \quad (31)$$

The tabulated values of R were computed from the boundary-layer solutions as follows:

$$R_v = \frac{K}{f''(0, \beta, K)} \quad (32)$$

$$R_T = \frac{K\Lambda_T}{\Pi'(0, \beta, K, \Lambda_T)} \quad (33)$$

$$R_{AB} = \frac{K\Lambda_{AB}}{\Pi'(0, \beta, K, \Lambda_{AB})} \quad (34)$$

and are constants over the mass-transfer surface. Thus the ratios N_{A0}/N_{B0}, N_{A0}/q_0, and $N_{A0}U/\tau_0$ are all constant with respect to x. This constancy results, of course, from the similarity properties of the profiles under the present boundary conditions.

Physically, the R quantities are the ratios of the momentum, energy and material fluxes by bulk flow at the surface to the corresponding fluxes by molecular agitation. These *flux ratios* occur prominently in many physical applications [6, 10, 12, 14, 17, 18]. It is clear from equations [26–28] that, for given geometry and physical properties, specification of any one of the four quantities K, R_v, R_T, R_{AB} determines all of them; any problem of this type can be solved directly from Table 1.

At high mass transfer rates toward the wall, the results in Table 1 converge toward the following asymptotes:

$$\lim_{K\to-\infty} f''(0) \to -K,$$

$$\lim_{K\to-\infty} \Pi'(0) \to -K\Lambda \quad (35, 36)$$

$$\lim_{K\to-\infty} R_v \to -1,$$

$$\lim_{K\to-\infty} R_T, R_{AB} \to -1. \quad (37, 38)$$

It should be noted that in this region the significant part of the tabulated quantities is their deviation from these asymptotes. Thus, if one inadvertently rounded off R to $-1{\cdot}0$ the predicted mass transfer rate would be infinite!

In the present calculations the quantities $\Pi'(0)$ and R_T or R_{AB} always lie *above* the asymptotes $-K\Lambda$ and -1, respectively. These conditions hold outside the region of reverse flow (see Fig. 2). The quantities $f''(0)$ and R_v lie

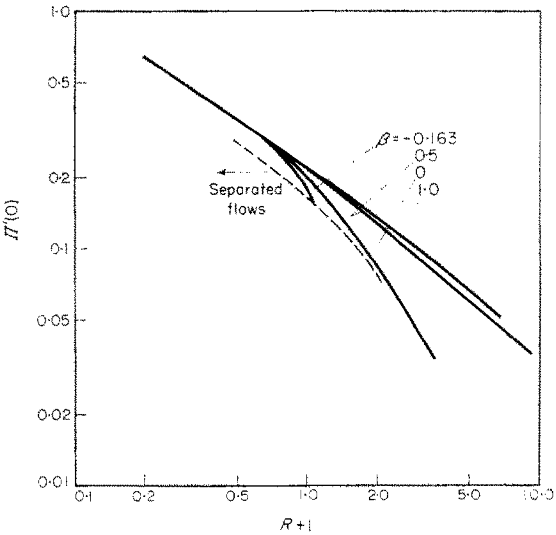

FIG. 3(a). Temperature or concentration gradients at the wall for $\Lambda = 0{\cdot}1$.

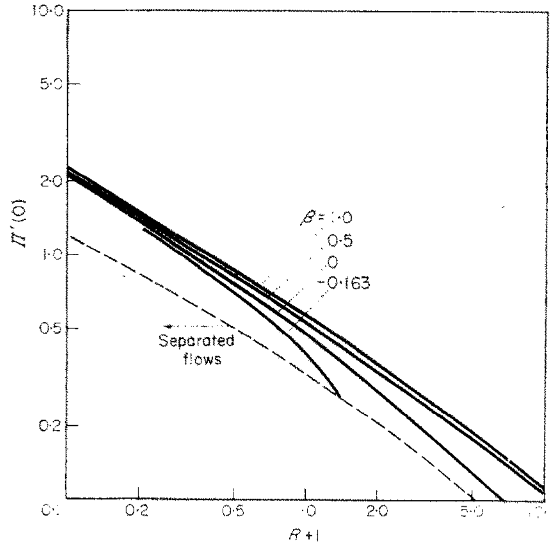

FIG. 3(b). Temperature or concentration gradients at the wall for $\Lambda = 1{\cdot}0$.

above their asymptotes if β is positive, but for negative β they may lie on either side, as can be seen from the behavior near the separation region.

Some sample plots of $\Pi'(0)$ versus $R + 1$ are given in Figs. 3(a), 3(b), and 3(c), to illustrate the behavior of the transfer coefficients. Clearly, mass transfer *into* the fluid *reduces* the transfer coefficients, whereas mass transfer *out of* the fluid *increases* the transfer coefficients. The dependence of $\Pi'(0)$ on the flow geometry is greatest near the separation limit.

Some additional boundary-layer parameters are given in Table 2, for use in the asymptotic calculations that follow. The dimensionless parameters D_0 and D_1 are defined by the equation

$$\lim_{\eta\to\infty} \int_0^\eta f \, d\eta = D_0 - D_1\eta + \tfrac{1}{2}\eta^2 \quad (39)$$

which describes the influence of the momentum boundary layer on the potential flow. The parameter D_1 has the further significance that

$$D_1 = \lim_{\eta\to\infty} \{\eta - f\} = \delta_p \sqrt{\left(\frac{m+1}{2}\,\frac{U}{\nu x}\right)} \quad (40)$$

in which δ_p is the distance the potential-flow streamlines are displaced in the y-direction as

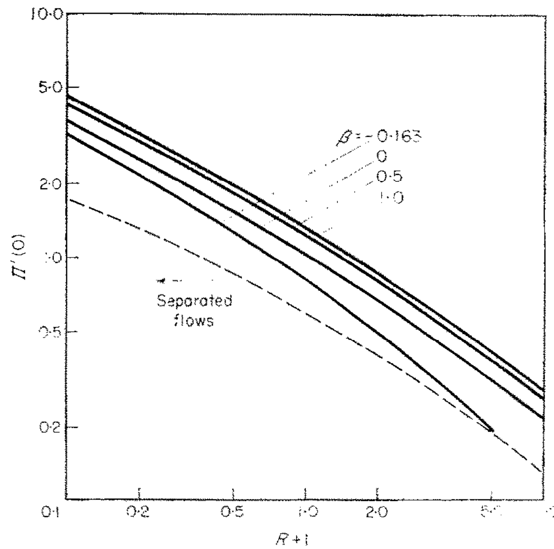

FIG. 3(c). Temperature or concentration gradients at the wall for $\Lambda = 10$.

compared with inviscid flow without mass transfer. Also included in Table 2, for all velocity profiles with injection ($K > 0$), are the position η_m at which f vanishes, and the coefficients needed to expand $\int_0^\eta f \, d\eta$ in powers of $\eta - \eta_m$.

The boundary-layer results for momentum transfer should be applicable for x/δ^* greater than about 10. The displacement thickness δ^* can be computed from the quantity D^* in Table 2. For heat transfer or diffusion, the same criterion may be used for Λ greater than about unity. The region of validity for the solutions for $\Lambda \ll 1$ is discussed in Section 4(c).

4. ASYMPTOTIC SOLUTIONS FOR HEAT TRANSFER AND DIFFUSION

For calculations outside the range of Table 1, and for some regions within it, the asymptotic solutions given here are useful. New results are given for four regions, based on four different methods of approximating the function $\int^\eta f \, d\eta$. For brevity we consider only the evaluation of $\Pi'(0)$ from equation (20), and do not discuss the complete profiles.

4(a) *Non-separated flows with large Λ and finite R*

If the thermal or diffusional boundary layer is thin enough, the Maclaurin expansion of f may be used in equation (20). This gives

$$\frac{1}{\Pi'(0)} = \int_0^\infty \exp\left[\Lambda K\eta - \frac{1}{6}\eta^3 \Lambda f_0'' - \frac{1}{24}\eta^4 \Lambda f_0''' - \frac{1}{120}\eta^5 \Lambda f_0^{\mathrm{iv}} - \frac{1}{720}\eta^6 \Lambda f_0^{\mathrm{v}} - \dots\right] d\eta. \quad (41)$$

For non-separated flows the transformation $w = \eta(\Lambda f_0'')^{1/3}$ is useful; this gives

$$\frac{(\Lambda f_0'')^{1/3}}{\Pi'(0)} = \int_0^\infty \exp\left[K_\infty w - \frac{1}{6}w^3 - \frac{1}{24}\Lambda^{-1/3}G_3 w^4 - \frac{1}{120}\Lambda^{-2/3}G_4 w^5 - \frac{1}{720}\Lambda^{-1}G_5 w^6 - \dots\right] dw \quad (42)$$

in which the following dimensionless quantities have been introduced:

$$K_\infty = \frac{\Lambda K}{(\Lambda f_0'')^{1/3}}, \quad G_3 = \frac{f_0'''}{f_0''^{4/3}}, \quad G_4 = \frac{f_0^{\mathrm{iv}}}{f_0''^{5/3}}, \quad G_5 = \frac{f_0^{\mathrm{v}}}{f_0''^{2}}. \quad (43)$$

Now the integrand in equation (42) may be partially expanded and integrated term by term to give the desired asymptotic series:

$$\begin{aligned}\frac{(\Lambda f_0'')^{1/3}}{\Pi'(0)} \simeq & \int_0^\infty \exp\left[K_\infty w - \frac{1}{6}w^3\right] dw \\ & + \Lambda^{-1/3}G_3 \int_0^\infty -\frac{w^4}{24}\exp\left[K_\infty w - \frac{1}{6}w^3\right] dw \\ & + \Lambda^{-2/3}G_3^2 \int_0^\infty \frac{w^2}{1152}\exp\left[K_\infty w - \frac{1}{6}w^3\right] dw \\ & + \Lambda^{-2/3}G_4 \int_0^\infty -\frac{w^5}{120}\exp\left[K_\infty w - \frac{1}{6}w^3\right] dw \\ & + \Lambda^{-1}G_3^2 \int_0^\infty -\frac{w^{12}}{82944}\exp\left[K_\infty w - \frac{1}{6}w^3\right] dw \\ & + \Lambda^{-1}G_3G_4 \int_0^\infty \frac{w^9}{2880}\exp\left[K_\infty w - \frac{1}{6}w^3\right] dw \\ & + \Lambda^{-1}G_5 \int_0^\infty -\frac{w^6}{720}\exp\left[K_\infty w - \frac{1}{6}w^3\right] dw \\ & + \dots \end{aligned} \quad (44)$$

Abbreviating the integrals and making use of equations (22) and (23), this becomes

$$\begin{aligned}\frac{R}{K_\infty} \equiv \frac{(\Lambda f_0'')^{1/3}}{\Pi'(0)} \simeq\ & I_0 \\ & + \Lambda^{-1/3}G_3 I_3 \\ & + \Lambda^{-2/3}[G_3^2 I_{33} + G_4 I_4] \\ & + \Lambda^{-1}[G_3^3 I_{333} + G_3G_4 I_{34} + G_5 I_5] \\ & + \dots \end{aligned} \quad (45)$$

The seven integrals, I_0 through I_5, are functions only of K_∞ and are given numerically in Table 3.

To use equation (45), one first specifies β and K and finds $f_0'' \equiv f''(0)$ from Table 1 or other published lists [7, 11, 13]. The desired higher derivatives of f are then found from equation (13) and its derivatives:

$$\left.\begin{aligned} f_0''' &= Kf_0'' - \beta \\ f_0^{\mathrm{iv}} &= Kf_0''' \\ f_0^{\mathrm{v}} &= Kf_0^{\mathrm{iv}} + (2\beta - 1)(f_0'')^2. \end{aligned}\right\} \quad (46)$$

Equation (45) may then be solved for either $\Pi'(0)$ or R.

Equation (45) converges asymptotically with increasing Λ, in non-separated flow, if K_∞ is maintained constant or if K is maintained at any

Table 2. Velocity-profile constants for use in asymptotic solutions

β	K	D_0	D_1	$D^* = D_1 - K$	F	G	H	η_m
1·0	− 5·0	0·03189	− 4·8189	0·1811	—	—	—	—
	− 3·0	0·06798	− 2·7329	0·2671	—	—	—	—
	− 1·0	0·1894	− 0·5407	0·4593	—	—	—	—
	− 0·5	0·2583	0·04233	0·5423	—	—	—	—
	− 0·2	0·3143	0·4026	0·6026	—	—	—	—
	− 0·1	0·3360	0·5247	0·6247	—	—	—	—
	0	0·3681	0·6500	0·6500	—	—	—	—
	0·1	0·3879	0·7729	0·6729	− 0·02868	0·4302	0·7983	0·4369
	0·2	0·4160	0·8985	0·6985	− 0·08449	0·5642	0·6315	0·6478
	0·5	0·5800	1·2981	0·7981	− 0·3695	0·7546	0·3682	1·1477
	1·0	0·7234	1·9450	0·9450	− 1·1974	0·8786	0·1889	1·8791
	2·0	1·4306	3·3616	1·3616	− 4·2300	0·9542	0·07247	3·3371
	3·0	2·6015	4·8608	1·8608	− 9·219	0·9760	0·03567	4·8462
0·5	− 5·0	0·03362	− 4·8141	0·1859	—	—	—	—
	− 3·0	0·07401	− 2·7183	0·2817	—	—	—	—
	− 1·0	0·2412	− 0·4768	0·5232	—	—	—	—
	− 0·5	0·3511	0·1413	0·6413	—	—	—	—
	− 0·2	0·4480	0·5328	0·7328	—	—	—	—
	− 0·1	0·4884	0·6677	0·7677	—	—	—	—
	0	0·5327	0·8048	0·8048	—	—	—	—
	0·1	0·5811	0·9443	0·8443	− 0·03298	0·3822	0·6579	0·5003
	0·2	0·6359	1·0868	0·8868	− 0·09746	0·5059	0·5461	0·7422
	0·5	0·8365	1·5309	1·0309	− 0·4318	0·6895	0·3610	1·3231
	1·0	1·3377	2·3340	1·3340	− 1·445	0·8151	0·2220	2·2138
	2·0	3·2891	4·1542	2·1542	− 5·388	0·9020	0·1197	4·0888
	3·0	6·4878	6·0834	3·0834	− 12·029	0·9361	0·02300	6·0499
0·0	− 5·0	0·03558	− 4·8087	0·1913	—	—	—	—
	− 3·0	0·08463	− 2·7004	0·2996	—	—	—	—
	− 1·0	0·3385	− 0·3691	0·6309	—	—	—	—
	− 0·5	0·5659	0·3398	0·8398	—	—	—	—
	− 0·2	0·8205	0·8349	1·0349	—	—	—	—
	− 0·1	0·9419	1·0191	1·1191	—	—	—	—
	0	1·0914	1·2168	1·2168	—	—	—	—
	0·1	1·2785	1·4314	1·3314	− 0·04684	0·2877	0·4177	0·7009
	0·2	1·5177	1·6681	1·4681	− 0·1430	0·3852	0·3813	1·0650
	0·5	2·8747	2·6118	2·1118	− 0·7523	0·5268	0·3151	2·1734
	0·75	7·0370	4·2377	3·4877	− 2·138	0·5776	0·2884	3·8526
	0·825	12·1844	5·5311	4·7061	− 3·305	0·5842	0·2841	5·1539
	0·85	17·0158	6·4778	5·6278	− 4·157	0·5860	0·2831	6·1025
	0·875	54·5507	11·1975	10·3225	− 8·333	0·5873	0·2824	10·8235
− 0·009115	0·75	13·2346	5·6932	4·9432	− 3·1739	0·5662	0·2896	5·2944
− 0·050178	0·5	6·5593	3·9021	3·4021	− 1·3024	0·4839	0·3065	3·3949
− 0·1	0	1·4558	1·4427	1·4427	—	—	—	—
	0·299685	4·7241	3·1538	2·8541	− 0·5613	0·3753	0·3081	2·4752
− 0·162793	− 1·0	0·3928	− 0·3135	0·6865	—	—	—	—
	− 0·5	0·7246	0·4693	0·9693	—	—	—	—
	− 0·2	1·1963	1·0931	1·2931	—	—	—	—
	− 0·1	1·4874	1·3673	1·4673	—	—	—	—
	0	1·9628	1·7252	1·7252	—	—	—	—
	0·1	3·6835	2·5975	2·4975	− 0·1148	0·1975	0·2586	1·5277

Table 2.—continued

β	K	D_0	D	$D^* = D_1 - K$	F	G	H	η_m
− 0·198838	0	3·3113	2·3588	2·3588	—	—	—	—
− 0·2	− 3·0	0·08911	− 2·6919	0·3081	—	—	—	—
	− 1·0	0·4087	− 0·2982	0·7018	—	—	—	—
	− 0·5	0·7784	0·5102	1·0102	—	—	—	—
	− 0·2	1·3636	1·1981	1·3981	—	—	—	—
	− 0·1	1·7959	1·5427	1·6427	—	—	—	—
	− 0·00309208	3·3002	2·3518	2·3549	—	—	—	—
− 0·237842	− 0·1	3·0033	2·1387	2·2387	—	—	—	—
− 0·422021	− 0·5	2·1661	1·3796	1·8796	—	—	—	—
− 0·5	− 0·64596487	1·9585	1·1351	1·7811	—	—	—	—
− 0·712061	− 1·0	1·5763	0·5867	1·5867	—	—	—	—
− 1·0	− 1·4142136	1·2692	0·0000	1·4142	—	—	—	—

negative value. That is, the error in the prediction of $\Pi'(0)$ or R, based on the first n terms of the series, vanishes as $\Lambda \to \infty$ for any $n \geqslant 1$. The asymptote for $\Lambda \to \infty$ with *constant positive* K (so that $K_\infty \to +\infty$) is given in Section 4(b).

Several previously known solutions are included in equation (45). Thus, when $K_\infty = 0$, equation (45) yields Merk's asymptotic series [19] for heat transfer (or diffusion) in non-separated flow. For a second example, when K_∞ is finite and Λ is large, equation (45) simplifies as follows:

as $\Lambda \to \infty$

$$R \to K_\infty I_0 \tag{47a}$$

at constant K_∞,

and by inversion of this relation,

as $\Lambda \to \infty$

at constant R, $K_\infty \to$ a function of R. (47b)

This asymptotic function, independent of β for non-separated flows, is given in Fig. 4 and in Table 3; it includes the earlier solution of Stewart and associates [17, 12, 14], and an equivalent solution by Merk [15], for flat-plate flow with $\Lambda \to \infty$. Finally, in the limit as $K_\infty \to 0$, equation (47a) becomes equivalent to Lighthill's solution [20] for heat transfer from an isothermal wedge:

as $\Lambda \to \infty$

$$R \to 1{\cdot}6227\, K_\infty \tag{48a}$$

and $K_\infty \to 0$,

or

$$\Pi'(0) \to \frac{(f_0''\Lambda)^{1/3}}{1{\cdot}6227}. \tag{48b}$$

These results are, of course, valid for diffusion as well.

Equation (45) has been tested against most of the exact solutions in Table 1, and a sample of the results is shown in Table 4. Results are also given for the method of Spalding and Evans [9], which was derived by integrating equations (20) with truncated parabolic velocity profiles. The

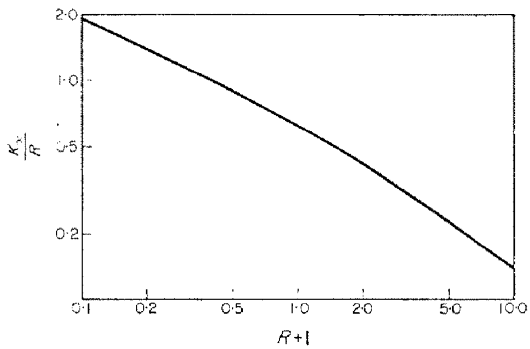

FIG. 4. Asymptotic solution for the heat and mass fluxes according to equations (60a, b).

Table 3. Integrals for equation (45).

K_∞	R at $\Lambda = \infty$	I_0	I_3	I_{33}	I_4	I_{333}	I_{34}	I_5
-4.00	-9.8618×10^{-1}	2.4655×10^{-1}	-6.716×10^{-4}	3.491×10^{-5}	-1.397×10^{-4}	-4.821×10^{-6}	2.249×10^{-5}	-2.794×10^{-5}
-3.00	-9.7087×10^{-1}	3.2362×10^{-1}	-2.078×10^{-3}	1.929×10^{-4}	-5.096×10^{-4}	-4.089×10^{-5}	1.398×10^{-4}	-1.184×10^{-4}
-2.50	-9.5497×10^{-1}	3.8199×10^{-1}	-3.940×10^{-3}	4.903×10^{-4}	-1.052×10^{-3}	-1.284×10^{-4}	3.768×10^{-4}	-2.637×10^{-4}
-2.00	-9.2674×10^{-1}	4.6337×10^{-1}	-7.907×10^{-3}	1.318×10^{-3}	-2.298×10^{-3}	-4.248×10^{-4}	1.073×10^{-3}	-6.218×10^{-4}
-1.90	-9.1869×10^{-1}	4.8352×10^{-1}	-9.155×10^{-3}	1.617×10^{-3}	-2.707×10^{-3}	-5.431×10^{-4}	1.332×10^{-3}	-7.435×10^{-4}
-1.80	-9.0955×10^{-1}	5.0531×10^{-1}	-1.063×10^{-2}	1.989×10^{-3}	-3.196×10^{-3}	-6.959×10^{-4}	1.656×10^{-3}	-8.911×10^{-4}
-1.70	-8.9913×10^{-1}	5.2890×10^{-1}	-1.237×10^{-2}	2.453×10^{-3}	-3.782×10^{-3}	-8.935×10^{-4}	2.065×10^{-3}	-1.071×10^{-3}
-1.60	-8.8723×10^{-1}	5.5452×10^{-1}	-1.443×10^{-2}	3.031×10^{-3}	-4.488×10^{-3}	-1.150×10^{-3}	2.581×10^{-3}	-1.290×10^{-3}
-1.50	-8.7358×10^{-1}	5.8239×10^{-1}	-1.688×10^{-2}	3.755×10^{-3}	-5.340×10^{-3}	-1.483×10^{-3}	2.233×10^{-3}	-1.557×10^{-3}
-1.40	-8.5791×10^{-1}	6.1279×10^{-1}	-1.980×10^{-2}	4.662×10^{-3}	-6.369×10^{-3}	-1.916×10^{-3}	4.060×10^{-3}	-1.885×10^{-3}
-1.30	-8.3986×10^{-1}	6.4604×10^{-1}	-2.328×10^{-2}	5.803×10^{-3}	-7.617×10^{-3}	-2.482×10^{-3}	5.109×10^{-3}	-2.288×10^{-3}
-1.20	-8.1900×10^{-1}	6.8250×10^{-1}	-2.746×10^{-2}	7.240×10^{-3}	-9.134×10^{-3}	-3.222×10^{-3}	6.445×10^{-3}	-2.784×10^{-3}
-1.10	-7.9484×10^{-1}	7.2259×10^{-1}	-3.247×10^{-2}	9.056×10^{-3}	-1.098×10^{-2}	-4.191×10^{-3}	8.150×10^{-3}	-3.397×10^{-3}
-1.00	-7.6678×10^{-1}	7.6678×10^{-1}	-3.851×10^{-2}	1.136×10^{-2}	-1.324×10^{-2}	-5.465×10^{-3}	1.033×10^{-2}	-4.155×10^{-3}
-0.95	-7.5106×10^{-1}	7.9059×10^{-1}	-4.198×10^{-2}	1.273×10^{-2}	-1.455×10^{-2}	-6.245×10^{-3}	1.164×10^{-2}	-4.600×10^{-3}
-0.90	-7.3408×10^{-1}	8.1564×10^{-1}	-4.580×10^{-2}	1.427×10^{-2}	-1.600×10^{-2}	-7.141×10^{-3}	1.312×10^{-2}	-5.095×10^{-3}
-0.85	-7.1572×10^{-1}	8.4203×10^{-1}	-5.000×10^{-2}	1.602×10^{-2}	-1.761×10^{-2}	-8.169×10^{-3}	1.481×10^{-2}	-5.648×10^{-3}
-0.80	-6.9587×10^{-1}	8.6984×10^{-1}	-5.462×10^{-2}	1.798×10^{-2}	-1.940×10^{-2}	-9.351×10^{-3}	1.672×10^{-2}	-6.265×10^{-3}
-0.75	-6.7437×10^{-1}	8.9916×10^{-1}	-5.971×10^{-2}	2.021×10^{-2}	-2.138×10^{-2}	-1.071×10^{-2}	1.888×10^{-2}	-6.954×10^{-3}
-0.70	-6.5109×10^{-1}	9.3012×10^{-1}	-6.533×10^{-2}	2.272×10^{-2}	-2.358×10^{-2}	-1.227×10^{-2}	2.134×10^{-2}	-7.724×10^{-3}
-0.65	-6.2584×10^{-1}	9.6283×10^{-1}	-7.152×10^{-2}	2.555×10^{-2}	-2.602×10^{-2}	-1.407×10^{-2}	2.413×10^{-2}	-8.585×10^{-3}
-0.60	-5.9844×10^{-1}	9.9740×10^{-1}	-7.836×10^{-2}	2.877×10^{-2}	-2.874×10^{-2}	-1.614×10^{-2}	2.731×10^{-2}	-9.549×10^{-3}
-0.55	-5.6869×10^{-1}	1.0[illegible]40	-8.592×10^{-2}	3.240×10^{-2}	-3.176×10^{-2}	-1.853×10^{-2}	3.092×10^{-2}	-1.063×10^{-2}
-0.50	-5.3636×10^{-1}	1.0727	-9.427×10^{-2}	3.652×10^{-2}	-3.513×10^{-2}	-2.128×10^{-2}	3.503×10^{-2}	-1.184×10^{-2}
-0.45	-5.0120×10^{-1}	1.1138	-1.035×10^{-1}	4.118×10^{-2}	-3.888×10^{-2}	-2.446×10^{-2}	3.971×10^{-2}	-1.319×10^{-2}
-0.40	-4.6294×10^{-1}	1.1573	-1.137×10^{-1}	4.647×10^{-2}	-4.306×10^{-2}	-2.812×10^{-2}	4.505×10^{-2}	-1.471×10^{-2}
-0.35	-4.2125×10^{-1}	1.2036	-1.251×10^{-1}	5.247×10^{-2}	-4.772×10^{-2}	-3.235×10^{-2}	5.113×10^{-2}	-1.641×10^{-2}
-0.30	-3.7582×10^{-1}	1.2527	-1.377×10^{-1}	5.929×10^{-2}	-5.293×10^{-2}	-3.724×10^{-2}	5.807×10^{-2}	-1.833×10^{-2}
-0.25	-3.2625×10^{-1}	1.3050	-1.516×10^{-1}	6.703×10^{-2}	-5.875×10^{-2}	-4.289×10^{-2}	6.599×10^{-2}	-2.048×10^{-2}
-0.20	-2.7212×10^{-1}	1.3606	-1.671×10^{-1}	7.583×10^{-2}	-6.525×10^{-2}	-4.942×10^{-2}	7.503×10^{-2}	-2.291×10^{-2}
-0.15	-2.1298×10^{-1}	1.4199	-1.843×10^{-1}	8.584×10^{-2}	-7.252×10^{-2}	-5.699×10^{-2}	8.537×10^{-2}	-2.563×10^{-2}
-0.10	-1.4831×10^{-1}	1.4831	-2.034×10^{-1}	9.724×10^{-2}	-8.066×10^{-2}	-6.574×10^{-2}	9.719×10^{-2}	2.870×10^{-2}
-0.05	-7.7528×10^{-1}	1.5506	2.247×10^{-1}	1.102×10^{-1}	-8.978×10^{-2}	-7.588×10^{-2}	1.107×10^{-1}	3.216×10^{-2}
0.00	0.0000×10^{-1}	1.6227	-2.484×10^{-1}	1.250×10^{-1}	-1.000×10^{-1}	8.764×10^{-2}	1.262×10^{-1}	-3.606×10^{-2}
0.05	8.4987×10^{-2}	1.6997	2.748×10^{-1}	1.419×10^{-1}	-1.115×10^{-1}	-1.013×10^{-1}	1.439×10^{-1}	-4.046×10^{-2}
0.10	1.7823×10^{-1}	1.7823	3.042×10^{-1}	1.611×10^{-1}	-1.243×10^{-1}	-1.171×10^{-1}	1.643×10^{-1}	-4.543×10^{-2}
0.15	2.8060×10^{-1}	1.8707	-3.371×10^{-1}	1.831×10^{-1}	-1.388×10^{-1}	-1.355×10^{-1}	1.876×10^{-1}	-5.104×10^{-2}
0.20	3.9310×10^{-1}	1.9655	3.738×10^{-1}	2.081×10^{-1}	-1.550×10^{-1}	-1.568×10^{-1}	2.144×10^{-1}	-5.739×10^{-2}
0.25	5.1682×10^{-1}	2.0673	-4.148×10^{-1}	2.368×10^{-1}	-1.733×10^{-1}	-1.816×10^{-1}	2.451×10^{-1}	-6.457×10^{-2}
0.30	6.5300×10^{-1}	2.1767	-4.606×10^{-1}	2.696×10^{-1}	-1.939×10^{-1}	-2.105×10^{-1}	2.804×10^{-1}	-7.270×10^{-2}
0.35	8.0301×10^{-1}	2.2943	-5.119×10^{-1}	3.071×10^{-1}	-2.170×10^{-1}	-2.441×10^{-1}	3.210×10^{-1}	-8.191×10^{-2}
0.40	9.6839×10^{-1}	2.4210	-5.694×10^{-1}	3.501×10^{-1}	-2.431×10^{-1}	-2.831×10^{-1}	3.677×10^{-1}	-9.235×10^{-2}
0.45	1.1509	2.5575	-6.338×10^{-1}	3.993×10^{-1}	-2.726×10^{-1}	-3.287×10^{-1}	4.214×10^{-1}	-1.042×10^{-1}
0.50	1.3524	2.7048	-7.060×10^{-1}	4.558×10^{-1}	-3.058×10^{-1}	-3.817×10^{-1}	4.833×10^{-1}	-1.176×10^{-1}
0.55	1.5751	2.8638	-7.871×10^{-1}	5.206×10^{-1}	-3.434×10^{-1}	-4.436×10^{-1}	5.546×10^{-1}	-1.329×10^{-1}
0.60	1.8215	3.0358	-8.781×10^{-1}	5.949×10^{-1}	-3.858×10^{-1}	-5.158×10^{-1}	6.369×10^{-1}	-1.503×10^{-1}
0.65	2.0942	3.2218	9.804×10^{-1}	6.803×10^{-1}	-4.337×10^{-1}	6.001×10^{-1}	7.317×10^{-1}	-1.700×10^{-1}
0.70	2.3964	3.4234	-1.095	7.785×10^{-1}	-4.880×10^{-1}	6.986×10^{-1}	8.413×10^{-1}	1.925×10^{-1}
0.75	2.7314	3.6419	-1.225	8.913×10^{-1}	-5.495×10^{-1}	-8.136×10^{-1}	9.678×10^{-1}	-2.180×10^{-1}
0.80	3.1033	3.8791	1.371	1.021	-6.192×10^{-1}	9.482×10^{-1}	1.114	-2.472×10^{-1}
0.85	3.5163	4.1369	-1.535	1.171	-6.983×10^{-1}	-1.106	1.283	-2.804×10^{-1}
0.90	3.9755	4.4172	1.721	1.343	-7.880×10^{-1}	-1.290	1.479	-3.184×10^{-1}
0.95	4.4863	4.7224	-1.930	1.542	-8.898×10^{-1}	-1.506	1.705	-3.617×10^{-1}
1.00	5.0551	5.0551	-2.167	1.771	-1.006	-1.759	1.968	-4.112×10^{-1}
1.10	6.3961	5.8146	-2.737	2.341	-1.287	-2.403	2.625	-5.325×10^{-1}
1.20	8.0671	6.7226	-3.468	3.102	-1.652	-3.292	3.511	-6.916×10^{-1}
1.30	1.0156×10^{1}	7.8125	4.408	4.122	-2.127	-4.518	4.706	-9.006×10^{-1}
1.40	1.2777×10^{1}	9.1265	-5.619	5.491	-2.746	-6.216	6.324	-1.176
1.50	1.6076×10^{1}	1.0717×10^{1}	-7.185	7.332	-3.556	-8.572	8.520	-1.540
1.60	2.0241×10^{1}	1.2651×10^{1}	9.217	9.816	-4.618	-1.185×10^{1}	1.151×10^{1}	-2.022
1.70	2.5519×10^{1}	1.5011×10^{1}	-1.186×10^{1}	1.317×10^{1}	-6.014	-1.641×10^{1}	1.557×10^{1}	-2.662
1.80	3.2227×10^{1}	1.7904×10^{1}	1.530×10^{1}	1.773×10^{1}	-7.855	-2.278×10^{1}	2.114×10^{1}	-3.515
1.90	4.0783×10^{1}	2.1465×10^{1}	-1.981×10^{1}	2.391×10^{1}	-1.029×10^{1}	-3.169×10^{1}	2.875×10^{1}	-4.654
2.00	5.1730×10^{1}	2.5865×10^{1}	-2.572×10^{1}	3.234×10^{1}	-1.352×10^{1}	-4.418×10^{1}	3.921×10^{1}	-6.178
2.50	1.7699×10^{2}	7.0794×10^{1}	-9.935×10^{1}	1.519×10^{2}	-5.518×10^{1}	-2.408×10^{2}	1.917×10^{2}	-2.653×10^{1}
3.00	6.5400×10^{2}	2.1800×10^{2}	-4.133×10^{2}	7.590×10^{2}	-2.417×10^{2}	-1.387×10^{3}	9.956×10^{2}	-1.218×10^{2}
4.00	1.1358×10^{4}	2.8395×10^{3}	-8.880×10^{3}	2.276×10^{4}	-5.698×10^{3}	-5.423×10^{4}	3.206×10^{4}	-3.128×10^{3}

Table 4. *Comparison of asymptotic solutions in Section* 4(a)

				Per cent error in predicted $\Pi'(0)$ at given K					
β	K	Λ	R	equation (45) 1 term	equation (45) 2 terms	equation (45) 4 terms	equation (45) 7 terms	Method of Ref. [9]	$\left(\frac{\partial \ln K}{\partial \ln R}\right)$
1·0	− 0·2	1·0	− 0·2844	13·67	2·72	− 0·35	− 0·25	− 3·24	1·25
		10.0	− 0·7307	2·66	0·29	0·06	0·09	− 0·09	2·37
	0·0	1·0	0·0000	15·84	3·82	− 0·13	− 0·23	− 2·88	1·00
		10·0	0·0000	6·45	1·02	0·12	0·11	− 0·20	1·00
	0·2	1·0	0·4447	18·42	5·21	0·19	− 0·17	− 2·11	0·80
		10·0	4·5334	15·84	3·46	0·44	0·06	− 0·27	0·42
0·0	− 0·2	1·0	− 0·3231	4·17	1·36	1·32	− 0·23	1·02	1·33
		10·0	− 0·7965	0·57	0·08	0·08	0·03	0·06	3·03
	0·0	1·0	0·0000	2·01	2·01	2·01	− 0·21	2·01	1·00
		10·0	0·0000	0·22	0·22	0·22	0·00	0·22	1·00
	0·2	1·0	0·6051	− 2·81	3·45	3·14	− 0·34	2·53	0·71
		10·0	10·50	− 6·28	1·72	1·18	− 0·10	0·76	0·30
− 0·2	− 0·2	1·0	− 0·3563	− 3·52	3·71	0·80	0·08	2·19	1·51
		10·0	− 0·8439	− 0·84	0·14	0·03	0·00	0·08	4·32
	− 0·1	1·0	− 0·2145	− 9·98	11·72	− 5·83	10·04	2·54	1·26
		10·0	− 0·6684	− 3·53	1·01	− 0·23	0·16	0·19	2·23

deviations listed are for predictions of $\Pi'(0)$ at the given β, K and Λ; multiplication of these deviations by the numbers in the last column gives the deviations expected in predicting K at the given values of β, R and Λ.

The results with 7 terms of equation (45) are generally the best, and could be further improved by use of Euler's transformation. The Spalding–Evans tables, and the two-term form of equation (45), both offer a good balance between simplicity and accuracy; hence it may prove useful to adapt one or both of these solutions to more general boundary-layer problems.

4(b) *Asymptote for large* Λ *with* $R \gg 1$

Under these conditions the integrand of equation (20) passes through a pronounced maximum at the position $\eta = \eta_m$ given in Table 2. The series in equation (41) may converge rather slowly for η as large as η_m, and it is then preferable to integrate equation (20) using an expansion in powers of $z = \eta - \eta_m$:

$$\int_0^\eta f\,\mathrm{d}\eta = \int_0^{\eta_m} f\,\mathrm{d}\eta + \frac{z^2}{2!} f'(\eta_m, \beta, K) + \frac{z^3}{3!} f''(\eta_m, \beta, K) + \ldots \quad (49)$$

In the notation of Table 2, this becomes:

$$\int_0^\eta f\,\mathrm{d}\eta = F + \frac{z^2}{2} G + \frac{z^3}{6} H + \ldots . \quad (50)$$

Insertion of the first two terms of this expansion into equation (20), and integration from $z = -\eta_m$ to $z = \infty$, yields the asymptotic formula:

$$\Pi'(0) \simeq \sqrt{\left(\frac{2G}{\pi}\right)} \frac{\exp(\Lambda F)}{1 + \mathrm{erf}\,[\eta_m \sqrt{(G\Lambda/2)}]}. \quad (51)$$

This formula is compared with exact calculations in Table 5. The predicted values of $\Pi'(0)$ are accurate within 2 per cent for $K > 0{\cdot}2$, and the corresponding accuracy for prediction of K at given R would be even better. Considering the simplicity of the formula, the accuracy is very gratifying.

In the limit as $\Lambda \to \infty$, at constant K_∞, equation (51) yields an asymptotic expansion of equation (47a) for large K_∞:

$$\lim_{\substack{\Lambda\to\infty \\ K_\infty \gg 1}} R \simeq \left(\frac{\pi^2 K_\infty^3}{8}\right)^{1/4} \exp\left(\frac{\sqrt{8}}{3} K_\infty^{3/2}\right) [1 + \mathrm{erf}\,(2^{1/4} K_\infty^{3/4})]. \quad (52)$$

Table 5. Comparison of equation (51) *with exact solutions*

			Values of $\Pi'(0)$	
β	K	Λ	Asymptotic equation (51)	Exact, Table 1
1·0	3·0	10	$1{\cdot}14 \times 10^{-40}$	$1{\cdot}14 \times 10^{-40}$
	2·0		$5{\cdot}25 \times 10^{-19}$	$5{\cdot}24 \times 10^{-19}$
	1·0		$7{\cdot}46 \times 10^{-6}$	$7{\cdot}42 \times 10^{-6}$
	0·5		$2{\cdot}73 \times 10^{-2}$	$2{\cdot}704 \times 10^{-2}$
	0·2		$4{\cdot}34 \times 10^{-1}$	$4{\cdot}412 \times 10^{-1}$
	0·1		$7{\cdot}60 \times 10^{-1}$	$8{\cdot}173 \times 10^{-1}$
0·5	3·0	10	$6{\cdot}9 \times 10^{-53}$	$6{\cdot}9 \times 10^{-53}$
	2·0		$4{\cdot}8 \times 10^{-24}$	$4{\cdot}8 \times 10^{-24}$
	1·0		$6{\cdot}05 \times 10^{-7}$	$6{\cdot}02 \times 10^{-7}$
	0·5		$1{\cdot}40 \times 10^{-2}$	$1{\cdot}376 \times 10^{-2}$
	0·2		$3{\cdot}56 \times 10^{-1}$	$3{\cdot}600 \times 10^{-1}$
	0·1		$6{\cdot}71 \times 10^{-1}$	$7{\cdot}201 \times 10^{-1}$
0·0	0·875	10	$6{\cdot}3 \times 10^{-37}$	$6{\cdot}2 \times 10^{-37}$
	0·75		$4{\cdot}96 \times 10^{-10}$	$4{\cdot}9 \times 10^{-10}$
	0·5		$4{\cdot}95 \times 10^{-4}$	$4{\cdot}88 \times 10^{-4}$
	0·2		$1{\cdot}91 \times 10^{-1}$	$1{\cdot}905 \times 10^{-1}$
	0·1		$4{\cdot}80 \times 10^{-1}$	$5{\cdot}105 \times 10^{-1}$

This predicts R within 2·1 per cent of the value in Table 3 for $K_\infty = 1$, and the agreement becomes exact as $K_\infty \to \infty$. It appears, then, that equation (51) should predict $R(\beta, K, \Lambda)$ within about 2 per cent for $\Lambda > 10$ and $R > 5$, over the range of β studied here. The equation should predict $K(\beta, R, \Lambda)$ within about 1 per cent in the same region.

4(c) *Asymptotes for $K \ll 0$*

At large mass transfer rates toward the wall, the velocity profiles asymptotically approach the function

$$f' \simeq 1 - e^{K\eta} \tag{53}$$

at all values of β. This asymptote was pointed out by Schlichting and Bussmann [1]. From this one obtains the related asymptotes:

$$f''(0, \beta, K) \simeq -K \tag{54}$$

$$\int_0^\eta f\,d\eta \simeq \frac{1}{K^2}(1 - e^{K\eta}) - \left(K - \frac{1}{K}\right)\eta + \tfrac{1}{2}\eta^2. \tag{55}$$

Comparison with Tables 1 and 2 indicates that equations (54) and (55) are reasonably accurate in the range $K \leqslant -3$. The values of $\Pi'(0)$ derived here will have a comparable region of validity.

Equations (20) and (55) then give:

$$\frac{1}{\Pi'(0)} \simeq \int_0^\infty \exp\left[\frac{\Lambda}{K^2}(e^{K\eta} - 1) + \Lambda\left(K - \frac{1}{K}\right)\eta - \tfrac{1}{2}\Lambda\eta^2\right] d\eta \tag{56}$$

which holds for any value of Λ, since equation (55) holds asymptotically for the whole range of η. Notice that the integral is independent of β; this is in approximate agreement with Table 1 for $K \leqslant -3$. Expanding the term $\Lambda\, e^{K\eta}/K^2$ in series and integrating, one obtains finally:

$$\frac{1}{\Pi'(0)} \simeq \sqrt{\left(\frac{\pi}{2\Lambda}\right)}\, e^{-\Lambda/K^2} \sum_{m=0}^{\infty} \frac{(\Lambda/K^2)^m}{m!} e^{X_m^2}(1 - \operatorname{erf} X_m) \tag{57}$$

in which

$$X_m = \left(-\frac{mK}{\Lambda} - K + \frac{1}{K}\right)\sqrt{\frac{\Lambda}{2}}. \tag{58}$$

Equation (57) is convergent for $\Lambda < \infty$ and $K < 0$. It is useful mainly for small Λ or large negative K, where the convergence is rapid.

A simpler expansion may be obtained by expanding the integrand of equation (56) in a different manner:

$$\frac{1}{\Pi'(0)} \simeq \int_0^\infty [1 - \frac{\Lambda\eta}{K} - \frac{\Lambda\eta^2}{2} - \frac{\Lambda}{K^2}(1 - e^{K\eta}) + \ldots]\, e^{\Lambda K\eta}\, d\eta. \tag{59}$$

The result is

$$\frac{1}{\Pi'(0)} \simeq -\frac{1}{K\Lambda} + \frac{1}{K^3\Lambda^2(1+\Lambda)} - \frac{6 + 15\Lambda + 10\Lambda^2}{K^5\Lambda^3(2+\Lambda)(1+\Lambda)^3} + \ldots \tag{60}$$

or

$$R \simeq -1 + \frac{1}{K^2\Lambda(1+\Lambda)} - \frac{6 + 15\Lambda + 10\Lambda^2}{K^4\Lambda^2(2+\Lambda)(1+\Lambda)^3} + \ldots. \tag{61}$$

Equation (60) is an asymptotic expansion of the function in equation (57), and provides close bounds for that function as $K \to -\infty$.

Equations (60) and (61) are closely related to a solution given by Acrivos [21] for rapid mass transfer toward an arbitrary two-dimensional surface. For wedge flows his result becomes:

$$\Pi'(0) \simeq \sqrt{\left[\frac{\Lambda}{(1+R)(1+\Lambda)}\right]} \tag{62}$$

which is obtainable from equation (61) by expanding K in powers of $(1 + R)$ and retaining only the first term. In using this formula K should always be calculated to see if the assumed velocity profile in equation (53) is adequate.

The comparisons in Table 6 show that equations (57) and (60) are quite accurate in the region $K < -1$ if the value of β lies well above the separation boundary in Fig. 2. For Λ greater than about unity, however, better accuracy is obtained with two or more terms of equation (45), or with the method of Spalding and Evans [9]. Notice that the comparisons are based on prediction of K at a given value of R; such comparisons provide the best test of accuracy when R is near -1.

4(d) *Asymptotes for small values of Λ*

If Λ is very small, as in heat flow through molten metals, then the exponential integrand in equation (20) changes slowly with η and the major contribution to the definite integral comes from outside the momentum boundary layer. Then, to a fair approximation, we can replace $\int_0^\eta f\,d\eta$ in equation (20) by its asymptotic form for large η as given in equation (39). Integration of the resulting expression gives:

$$\Pi'(0) \simeq \sqrt{\left(\frac{2\Lambda}{\pi}\right)}\,\frac{\exp\left[D_0\Lambda - \frac{1}{2}D_1^2\Lambda\right]}{\left[1 + \operatorname{erf} D_1\sqrt{(\Lambda/2)}\right]}. \tag{63}$$

The quantities D_0 and D_1 are functions of β and K (see Table 2). The approximation to $\int_0^\eta f\,d\eta$ used here is an upper bound over the whole range of η, and consequently equation (63) gives an upper bound for $\Pi'(0)$ for any value of Λ.

In the region $K \ll 0$, the constants D_0 and

Table 6. *Comparison of exact and asymptotic solutions when $K \ll 0$*

β	K	Λ	R	Per cent errors in prediction of K at given R: equation (56)	equation (62)	equation (45) 2 terms	Method of Reference [9]
1·0	−1	0·1	−0·3418	−8·7[b]	27·0	6·9	−15·4
−0·2	−1	0·1	−0·3554	−4·1[b]	33·5	5·8	−10·8
1·0	−1	1·0	−0·7556	−15·4[b]	8·1	0·8	−7·2
−0·2	−1	1·0	−0·7880	−5·2[b]	21·0	0·1	−3·6
1·0	−1	10·0	−0·98630	−19·7[a]	−19·7	2·9	2·7
−0·2	−1	10·0	−0·990547	−2·8[a]	−2·9	−0·2	−0·3
1·0	−3	0·1	−0·6652	−1·6[b]	15·5	−9·1	−21·1
−0·2	−3	0·1	−0·6688	−0·6[b]	16·8	−9·1	−21·5
1·0	−3	1·0	−0·95143	−4·6[b]	1·8	−9·5	−11·6
−0·2	−3	1·0	−0·95446	−1·1[b]	5·4	−8·8	−11·1
1·0	−3	10·0	−0·998835	−7·3[a]	−7·0	−0·6	−0·6
−0·2	−3	10·0	−0·999022	1·2[a]	1·5	1·7	1·7
1·0	−5	0·1	−0·8048	−0·6[b]	9·8	−38·6	−23·2
0·0	−5	0·1	−0·8057	−0·2[b]	10·2	−38·1	−23·5
1·0	−5	1·0	−0·98101	−2·0[a,b]	0·7	−21·7	−13·0
0·0	−5	1·0	−0·98149	−0·7[a,b]	2·0	−20·7	−12·9
1·0	−5	10·0	−0·999613	−3·3[a]	−3·1	−0·7	−0·7
0·0	−5	10·0	−0·999631	−1·0[a]	−0·8	−0·4	−0·4

[a] Integral calculated from asymptotic series, equation (60).
[b] Integral calculated from convergent series, equation (57).

Table 7. Comparison of exact and asymptotic solutions for $\Lambda \ll 1$

β	K	Λ	R	Per cent error in prediction of $\Pi'(0)$ at given K		$\left(\frac{\partial \ln K}{\partial \ln R}\right)_{\beta, \Lambda}$
				equation (63)	equation (64)	
1·0	− 1·0	0·1	− 0·3418	0·21	1·68	1·34 [b]
		0·2	− 0·4522	0·59	3·16	1·52
		0·5	− 0·6237	2·41	6·85	1·96
	0·0	0·1	0·0	0·41	− 3·23	1·00
	1·0	0·1	0·6559	0·72	− 6·30	0·70
0·0	− 1·0	0·1	− 0·3514	0·42	− 2·92	1·39
	0·0	0·006	0·0	0·02 [a]	− 0·64 [a]	1·00
		0·01	0·0	0·05 [a]	− 1·03 [a]	1·00
		0·03	0·0	0·25 [a]	− 3·02 [a]	1·00
		0·1	0·0	0·20	− 10·15	1·00
	0·75	0·1	0·7270	10·66	− 45·25	0·31
− 0·198838 (Separation)	0·0	0·1	0·0	5·45	− 24·30	1·00

[a] The exact solutions for these three conditions were taken from Sparrow and Gregg [23].
[b] Multiplication of the tabulated errors by the factors in this column gives the expected errors in prediction of K at the given β, Λ and R.

D_1 can be estimated from equation (55), and equation (63) then becomes equivalent to the first term of equation (57). It is also interesting to note that for $K \gg 0$, equation (63) bears a resemblance to equation (51), which holds for $\Lambda \to \infty$.

A closely related solution for small Λ was given by Merk [19]. His result corresponds to equation (63) without the quantity D_0:

$$\Pi'(0) \simeq \sqrt{\left(\frac{2\Lambda}{\pi}\right)} \frac{\exp(-\frac{1}{2} D_1^2 \Lambda)}{[1 + \operatorname{erf} D_1 \sqrt{(\Lambda/2)}]}. \quad (64)$$

Merk's solution did not include mass transfer, but is easily extended to mass-transfer problems by obtaining D_1 from Table 2 at the desired β and K. A series solution consistent with equation (64) was given earlier by Morgan *et al.* [22], and was tested by Sparrow and Gregg [23] who gave exact calculations for the flat plate at small Prandtl numbers (see Table 7).

In Table 7 equations (63) and (64) are compared with exact calculations. Equation (63) is clearly superior, especially for flows with separation or injection.

For Λ less than about unity, longitudinal heat conduction or diffusion determines the region of x in which the boundary-layer solutions for $\Pi'(0)$ are useful. Estimation of a median Π-profile thickness consistent with equation (63) or (64) gives the region of applicability as

$$D_1 + \sqrt{[D_1^2 + (0{\cdot}5/\Lambda)]} < 0{\cdot}1 \sqrt{\left(\frac{m+1}{2} \frac{Ux}{\nu}\right)} \quad (65)$$

for laminar flow with $\Lambda \ll 1$.

5. CONCLUSION

The results in Sections 3 and 4 provide fairly complete information on momentum, heat and mass transfer rates in steady constant-property wedge flows. Naturally, modifications will be necessary to cope with problems involving more complicated geometries, variable properties, or multicomponent diffusion. These modifications will be treated in later papers in this series. Attention is also drawn to the works of Eckert and Livingood [6], Merk [19], and Spalding and Evans [7, 8, 9, 18] on some of these matters.

ACKNOWLEDGEMENTS

The authors wish to acknowledge the financial support received from the Wisconsin Alumni Research Foundation and the Sinclair Refining Company, and the cooperation extended by the staff of the University of Wisconsin Numerical Analysis Laboratory, during the course of this work.

REFERENCES

1. H. SCHLICHTING and K. BUSSMANN, Exakte Lösungen für die laminare Reibungsschicht mit Absaugung und Ausblasen. *Schriften Dtsch. Akad. Luftfahrtforsch.* 7B, Heft 2 (1943).
2. H. SCHAEFER, Laminare Grenzschicht zur Potentialströmung $U = u_1 x^m$ mit Absaugung und Ausblasen. *Dtsch. Luftfahrtforsch.* UM 2043 (1944).
3. E. R. G. ECKERT, Heat transfer and temperature profiles in laminar boundary layers on a sweat-cooled wall. Technical Report No. 5646. Air Materiel Command (1947).
4. H. SCHUH, Über die Lösung der laminaren Grenzschichtgleichung an einer ebenen Platte für Geschwindigkeits- und Temperaturfeld bei veränderlichen Stoffwerten und für das Diffusionsfeld bei höheren Konzentrationen. *Z. Angew. Math. Mech.* **25–27**, 54 (1947).
5. W. B. BROWN and P. L. DONOUGHE, Tables of exact laminar-boundary-layer solutions when the wall is porous and fluid properties are variable. *N.A.C.A. Tech. Note* 2479 (1951).
6. E. R. G. ECKERT and J. N. B. LIVINGOOD, Method for calculation of laminar heat transfer in air flow around cylinders of arbitrary cross-section (including large temperature differences and transpiration cooling). *N.A.C.A. Tech. Rep.* 1118 (1953).
7. D. B. SPALDING, Mass transfer through laminar boundary layers—1. The velocity boundary layer. *Int. J. Heat Mass Transfer*, **2**, 15 (1961).
8. D. B. SPALDING and H. L. EVANS, Mass transfer through laminar boundary layers—2. Auxiliary functions for the velocity boundary layer, *Int. J. Heat Mass Transfer*, **2**, 199 (1961).
9. D. B. SPALDING and H. L. EVANS, Mass transfer through laminar boundary layers—3. Similar solutions of the *b*-equation, *Int. J. Heat Mass Transfer*, **2**, 314 (1961).
10. J. P. HARTNETT and E. R. G. ECKERT, Mass transfer cooling in a laminar boundary layer with constant properties. University of Minnesota Heat Transfer Laboratory Technical Report No. 4 (1955).
11. H. W. EMMONS and D. C. LEIGH, Tabulation of the Blasius Function with suction and blowing. Interim Technical Report No. 9, Combustion Aerodynamics Laboratory, Harvard University (1953).
12. H. S. MICKLEY, R. C. ROSS, A. L. SQUYERS and W. E. STEWART, Heat, mass and momentum transfer for flow over a flat plate with blowing or suction. *N.A.C.A. Tech. Note* 3208 (1954).
13. J. N. B. LIVINGOOD and P. L. DONOUGHE, Summary of laminar-boundary-layer solutions for wedge-type flow over convection and transpiration-cooled surfaces. *N.A.C.A. Tech. Note* 3588 (1955).
14. R. B. BIRD, W. E. STEWART and E. N. LIGHTFOOT, *Transport Phenomena*, Chaps. 19, 21. Wiley, New York (1960).
15. H. J. MERK, Mass transfer in laminar boundary layers calculated by means of a perturbation method, *Appl. Sci. Res.* **A8**, 237 (1959).
16. H. SCHLICHTING, *Boundary Layer Theory*, Chap. 13. McGraw-Hill, New York (1960).
17. W. E. STEWART, Interaction of heat, mass and momentum transfer. Sc. D. Thesis, Massachusetts Institute of Technology (1951).
18. D. B. SPALDING, A standard formulation of the steady convective mass-transfer problem, *Int. J. Heat Mass Transfer*, **1**, 192 (1960).
19. H. J. MERK, Rapid calculations for boundary-layer transfer using wedge functions and asymptotic expansions, *J. Fluid Mech.* **5**, 460 (1959).
20. M. J. LIGHTHILL, Contributions to the theory of heat transfer through a laminar boundary layer, *Proc. Roy. Soc.* **A202**, 359 (1950).
21. A. ACRIVOS, Mass transfer in laminar-boundary-layer flows with finite interfacial velocities, *J. Amer. Inst. Chem. Engrs* **6**, 410 (1960).
22. G. W. MORGAN, A. C. PIPKIN and W. H. WARNER, On heat transfer in laminar boundary-layer flows of liquids having a very small Prandtl number, *J. Aero. Sci.* **25**, 173 (1958).
23. E. M. SPARROW and J. L. GREGG, Summary of low-Prandtl-number heat-transfer results for forced convection on a flat plate, *J. Aero. Sci.* **24**, 852 (1957).

Résumé—Les solutions de couche limite sont données pour l'écoulement de mélanges binaires à propriétés constantes, sur des plans et des dièdres avec transport de chaleur et de masse à la frontière. Les solutions numériques exactes sont données pour des nombres de Prandtl et de Schmidt de 0,1 à 10. Les solutions asymptotiques sont données pour des nombres de Prandtl et de Schmidt hors de ce domaine ainsi que pour des coefficients élevés de transport de masse vers la surface.

Zusammenfassung—Die Grenzschichtgleichungen sind angegeben für die Strömung binärer Gemische konstanter Stoffeigenschaften über ebene Flächen und Keile mit Warme- und Stoffübergang durch die Grenzflächen. Für Prandtl- und Schmidt-Zahlen von 0,1 bis 10 liegen exakte numerische Lösungen vor. Asymptotische Lösungen sind gültig für Prandtl- und Schmidt-Zahlen ausserhalb dieses Bereichs und für grosse Stoffübergangsgeschwindigkeiten.

Аннотация—Приводятся решения задачи переноса в пограничном слое для потока бинарных смесей с постоянными физическими свойствами на плоскостях клина при наличии тепло-и массообмена. Даются точные численные решения для чисел Прандтля и Шмидта в пределе от 0,1 до 10. Приводятся асимпточеские решения для чисел Прандтля и Шмидта вне этого предела, а также для больших скоростей массообмена по направлению к поверхности.